

VEGF-Induced Vascular Permeability Is Mediated by FAK

Xiao Lei Chen,^{1,5} Ju-Ock Nam,^{1,4,5} Christine Jean,¹ Christine Lawson,¹ Colin T. Walsh,¹ Erik Goka,^{1,6} Ssang-Taek Lim,¹ Alok Tomar,¹ Isabelle Tancioni,¹ Sean Uryu,¹ Jun-Lin Guan,³ Lisette M. Acevedo,² Sara M. Weis,² David A. Cheresh,² and David D. Schlaepfer^{1,*}

¹Department of Reproductive Medicine

²Department of Pathology

Moore's UCSD Cancer Center, La Jolla, CA 92093, USA

³Department of Internal Medicine-MMG, University of Michigan Medical School, Ann Arbor, MI 48108, USA

⁴Kyungpook National University, 386 Gajang-dong, Sangju-si, Gyeongsangbuk-Do 742-711, Korea

⁵These authors contributed equally to this work

⁶Present address: Miller School of Medicine, University of Miami, Miami, FL 33136, USA

*Correspondence: dschlaepfer@ucsd.edu

DOI 10.1016/j.devcel.2011.11.002

SUMMARY

Endothelial cells (ECs) form cell-cell adhesive junctional structures maintaining vascular integrity. This barrier is dynamically regulated by vascular endothelial growth factor (VEGF) receptor signaling. We created an inducible knockin mouse model to study the contribution of the integrin-associated focal adhesion tyrosine kinase (FAK) signaling on vascular function. Here we show that genetic or pharmacological FAK inhibition in ECs prevents VEGF-stimulated permeability downstream of VEGF receptor or Src tyrosine kinase activation *in vivo*. VEGF promotes tension-independent FAK activation, rapid FAK localization to cell-cell junctions, binding of the FAK FERM domain to the vascular endothelial cadherin (VE-cadherin) cytoplasmic tail, and direct FAK phosphorylation of β -catenin at tyrosine-142 (Y142) facilitating VE-cadherin- β -catenin dissociation and EC junctional breakdown. Kinase inhibited FAK is in a closed conformation that prevents VE-cadherin association and limits VEGF-stimulated β -catenin Y142 phosphorylation. Our studies establish a role for FAK as an essential signaling switch within ECs regulating adherens junction dynamics.

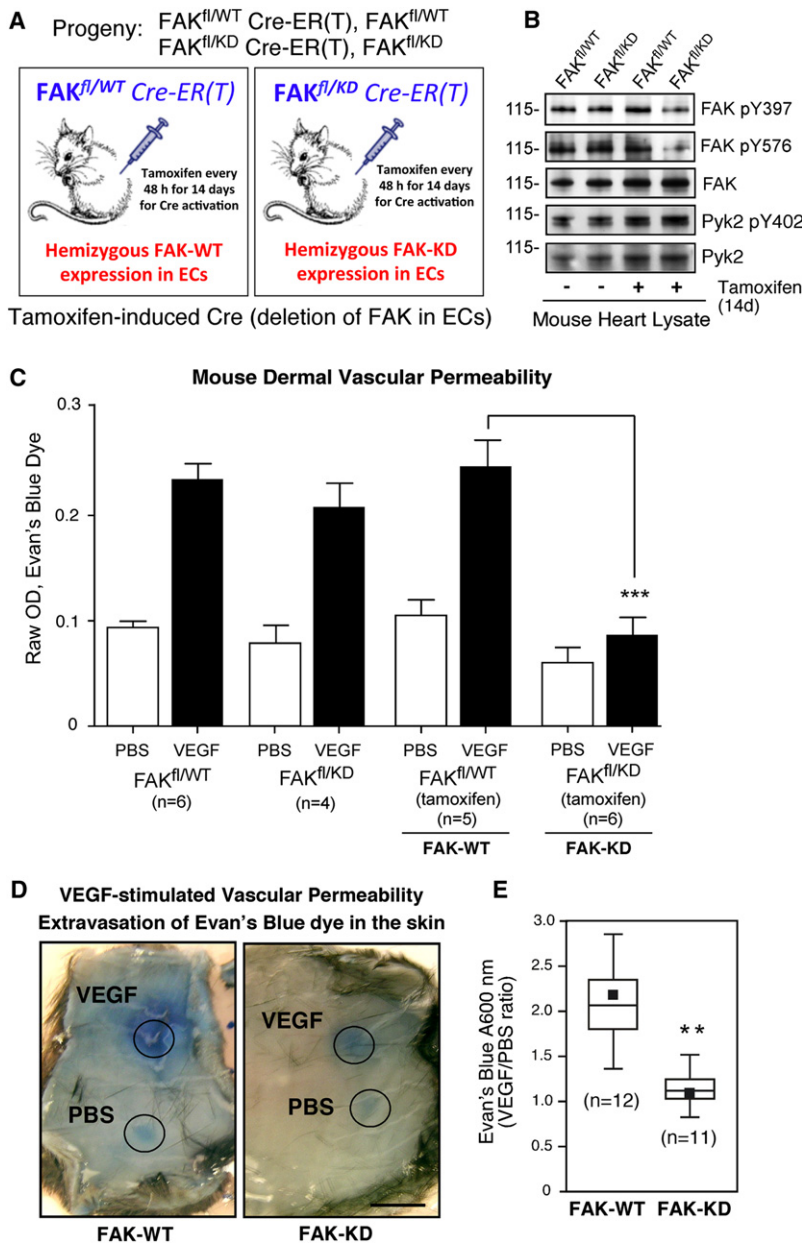
INTRODUCTION

Vascular barrier integrity can be disrupted by a variety of soluble permeability factors, and changes in barrier function can exacerbate tissue damage during cancer and ischemia (Weis and Cheresh, 2005). Endothelial cell-cell contacts create a vascular barrier that is regulated in part by the stability of cell-cell adherens junctional protein complexes (Nelson, 2008). Adherens junction (AJ) proteins such as VE-cadherin, β -catenin, p120-catenin, and α -catenin are critically involved in controlling vascular permeability (Dejana et al., 2008). Enhanced phosphorylation, endocytosis, S-nitrosylation, or cleavage of AJ proteins

facilitates endothelial cell (EC) barrier breakdown that can be triggered by growth factor receptor activation (Dejana et al., 2009; Harris and Nelson, 2010).

Vascular endothelial growth factor (VEGF) promotes vascular leak, angiogenesis, and the tyrosine phosphorylation of VE-cadherin and β -catenin (Dejana et al., 2008; Ferrara et al., 2003; Lilien and Balsamo, 2005). Mechanistically, knockout and pharmacological inhibitor studies point to the importance of Src-family protein-tyrosine kinase (PTK) activation by VEGF in promoting AJ phosphorylation (Eliceiri et al., 1999; Weis et al., 2004a). Interestingly, Src-family PTKs are also activated by integrin receptors that cross-talk with VEGF in the control of vascular permeability (De et al., 2005; Wang et al., 2006). The regulation of AJ stability is complicated as Src-mediated phosphorylation of VE-cadherin at tyrosine (Y) Y658, Y731 (Adam et al., 2010), or β -catenin phosphorylation at Y654 (Tominaga et al., 2008) are not singularly sufficient to disrupt barrier function. However, β -catenin Y142 phosphorylation disrupts α -catenin binding and mutation of this site prevents AJ formation (Piedra et al., 2003; Tominaga et al., 2008). Although Fer, Fyn, and PTK6 can phosphorylate β -catenin Y142 *in vitro* (Palka-Hamblin et al., 2010; Piedra et al., 2003), the regulation of Y142 β -catenin phosphorylation *in vivo* remains unknown.

Another PTK activated by VEGF and integrins is focal adhesion kinase (FAK) (Abedi and Zachary, 1997). FAK is comprised of an N-terminal FERM (band 4.1, ezrin, radixin, moesin homology (FERM) domain, central PTK region, and a C-terminal domain that links FAK to integrins (Mitra et al., 2005). VEGF can increase FAK phosphorylation at Y397, Y407, and Y861 through undefined mechanisms (Abu-Ghazaleh et al., 2001; Herzog et al., 2011) and VEGF-stimulated FAK Y397 phosphorylation occurs independently of Src (Liang et al., 2010). FAK phosphorylation at Y576 in the kinase domain activation loop is a marker of FAK activation (Mitra et al., 2005). In culture, VEGF triggers FAK binding to paxillin, FAK localization to nascent adhesions, and the formation of a FAK/ α v β 5 integrin signaling complex associated with the generation of actin-myosin tension and increased cell motility (Avraham et al., 2003; Birukova et al., 2009; Eliceiri et al., 2002). Expression of dominant-negative FAK prevents VEGF-stimulated permeability *in vitro* and in coronary vessels *ex vivo* through undetermined mechanisms (Wu et al., 2003).



Global or EC-specific FAK knockout mice show developmental vascular defects (Braren et al., 2006; Ilic et al., 2003; Shen et al., 2005). Vascular morphogenesis abnormalities are also associated with Y397 FAK deleted (Corsi et al., 2009) or FAK kinase-dead (KD) knockin mice (Lim et al., 2010a; Zhao et al., 2010). Although pharmacological FAK inhibition (Weis et al., 2008) or conditional FAK knockout in ECs (Tavora et al., 2010) prevents VEGF-associated angiogenesis and tumor-induced vascular permeability (Lee et al., 2010), the signaling connections for FAK in mediating these effects remain unclear. However, as basal VE-cadherin Y658 phosphorylation was reduced by loss of FAK expression or activity within ECs in culture (Zhao et al., 2010), we set out to define the role of FAK activity in VEGF-stimulated permeability.

Figure 1. FAK Activity within ECs Is Required for VEGF-Initiated Vascular Permeability in Mice

(A) Progeny from FAK^{fl/fl} SCL-Cre-ER(T) and heterozygous FAK^{KD/WT} crosses are treated with tamoxifen to induce Cre expression to create mice with hemizygous FAK-WT or FAK-KD expression in ECs. (B) Tamoxifen treatment of Cre-ER(T)-positive FAK^{fl/WT} and FAK^{fl/KD} mice results in reduced FAK pY397 and FAK pY576 phosphorylation but no changes in Pyk2 expression or Pyk2 pY402 phosphorylation in FAK^{fl/KD} compared to FAK^{fl/WT} mice by immunoblotting of heart lysates. (C) VEGF-stimulated dermal vascular permeability (VP) was measured in Cre-ER(T)-positive FAK^{fl/WT} and FAK^{fl/KD} mice with or without tamoxifen pretreatment. Leakage of circulating Evans blue dye was measured after 30 min. Shown are mean values \pm SEM (** $p < 0.001$). (D) Representative images of dermal dye leakage. VEGF or PBS injection sites are circled. Scale bar represents 0.5 cm. (E) Quantification of VP. Data is plotted as a VEGF/PBS ratio of individual mice from two independent experiments. Box-whisker plots show the distribution of the data: black square, mean; bottom line, 25th percentile; middle line, median; top line, 75th percentile; and whiskers, 5th and 95th percentiles (** $p < 0.01$). See also Figure S1.

Here, we report the generation of a knockin mouse model hemizygous for FAK wild-type (WT) or FAK-KD expression within adult ECs. FAK-KD vessels are phenotypically normal, but genetic or pharmacological FAK inhibition prevents VEGF-induced vascular permeability. VEGF triggers FAK activation in vivo leading to FAK FERM binding to VE-cadherin at cell-cell junctions and direct phosphorylation of β -catenin Y142 associated with AJ disassembly. These studies establish the importance of FAK activity in AJ regulation and support the use of FAK inhibitors in the treatment of vascular disease.

RESULTS

Creation of an Inducible FAK-KD Knockin Mouse

To assess the role of FAK signaling in vivo, we used a Cre/loxP strategy to create a conditional FAK-KD knockin within adult mouse ECs. This was accomplished by crossing homozygous floxed (fl) FAK mice containing an estrogen receptor tamoxifen [ER(T)] fusion driven by the 5' endothelial enhancer of the stem cell leukemia locus (Weis et al., 2008) with heterozygous FAK-KD knockin (FAK^{KD/WT}) mice (Figure S1A available online). Mouse model functionality was verified by staining for β -galactosidase (β -gal) in whole or sectioned hearts of mice crossed onto a *Rosa26 LacZ* reporter background (Figures S1B and S1C). EC-specific β -gal expression was detected only in tamoxifen-treated Cre-ERT mice. Tamoxifen promotes Cre-mediated excision of the floxed FAK allele, yielding mice with hemizygous FAK-WT or FAK-KD expression in ECs (Figure 1A). Phosphospecific blotting of heart lysates (enriched in ECs) was used to determine changes in FAK

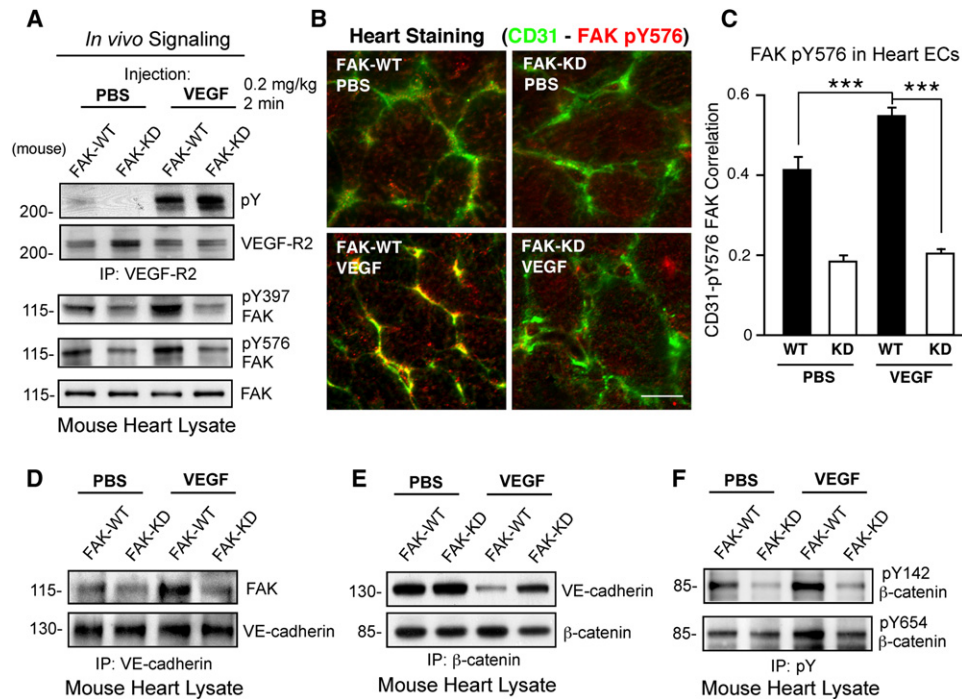


Figure 2. FAK-KD Prevents VEGF-Stimulated FAK Activation, FAK Association with VE-Cadherin, and β -Catenin Y142 Phosphorylation In Vivo

Hearts of tamoxifen-treated FAK^{fl/WT} (FAK-WT) or FAK^{fl/KD} (FAK-KD) mice were analyzed 2 min after VEGF (0.2 mg/kg) or PBS tail vein injections. (A) VEGF-R2 immunoprecipitation (IP) shows equal phosphotyrosine (pY) content after VEGF administration. Reduced FAK Y397 and Y576 phosphorylation after VEGF stimulation of FAK-KD compared to FAK-WT mice. (B) Heart sections were analyzed by combined staining for ECs (CD31, green) and activated FAK (pY576, red). Shown are merged images with FAK activation occurring within ECs (yellow) upon VEGF stimulation of FAK-WT but not FAK-KD mice. Scale bar represents 20 μ m. (C) Mean correlation of pixel intensities of CD31 to pY576 FAK staining from ten full frame images of experimental groups in (B) (\pm SEM, *** p < 0.001). (D) Increased VE-cadherin/FAK association after VEGF stimulation in FAK-WT but not FAK-KD heart lysates. (E) A VE-cadherin/ β -catenin complex is maintained in heart lysates upon VEGF stimulation of FAK-KD but not FAK-WT mice by IP analyses. (F) FAK-KD blocks basal and VEGF-stimulated β -catenin Y142 but not basal Y654 phosphorylation in heart lysates by anti-pY IP analyses. See also Figure S2.

activation since FAK-KD is not tagged. Upon tamoxifen treatment, FAK^{fl/KD} mice exhibited reduced FAK Y397 and Y576 phosphorylation compared to FAK^{fl/WT} mice (Figure 1B). In tamoxifen-treated FAK^{fl/WT} and FAK^{fl/KD} mice, there were no differences in total FAK, Pyk2, or Pyk2 phosphorylation in heart lysates (Figure 1B) or blood vessel density, size, or branching as determined by fluorescent lectin staining (Figure S1D). These results show that FAK-KD expression in adult mice inhibits FAK phosphorylation in vivo without gross alterations in vascular structure.

FAK-KD in ECs Prevents VEGF-Induced Vascular Permeability

As conditional loss of FAK expression decreases tumor- (Lee et al., 2010) and VEGF-induced (Weis et al., 2008) vascular permeability (VP), Cre-ERT-positive FAK^{fl/WT} and FAK^{fl/KD} mice with or without tamoxifen pretreatment were evaluated for dermal blood vessel-associated changes in VEGF-induced VP (Figure 1C). The leak of circulating Evan’s blue dye in the skin of mice was increased 2-fold by local injection of recombinant VEGF compared to control PBS injections (Figure 1D). Notably, tamoxifen-treated FAK^{fl/KD} (FAK-KD) mice exhibited significantly reduced leak compared to FAK^{fl/WT} (FAK-WT) mice (Figure 1C,

p < 0.001). Independent experiments revealed a 2-fold greater VEGF-stimulated leak in tamoxifen-treated FAK-WT compared to FAK-KD mice (Figure 1E, p < 0.01). These results support the importance of FAK signaling within ECs for VP initiation in vivo by VEGF.

FAK-KD Prevents VEGF-Stimulated FAK Activation In Vivo

To determine the molecular basis for FAK-KD effects on VEGF-induced VP, in vivo signaling assays were performed by immunoblotting or staining of hearts harvested after tail vein injection of VEGF or PBS (Figure 2). Equal VEGF receptor (VEGF-R2) tyrosine phosphorylation occurred in FAK-WT and FAK-KD mice whereas basal and VEGF-stimulated FAK Y397 and Y576 phosphorylation were reduced in FAK-KD mice (Figure 2A). VEGF triggered FAK activation within ECs as detected by costaining of heart sections with EC-specific (anti-CD31) and pY576 FAK antibodies (Figures 2B and S2A). Image analyses revealed a significant increase in overlapping CD31-pY576 FAK staining in heart tissues upon VEGF administration to FAK-WT mice (Figure 2C, p < 0.001). In FAK-KD mice, pY576 FAK levels were low and did not change upon VEGF stimulation (Figures 2B and 2C). Unexpectedly, neither Src nor Pyk2 phosphorylation

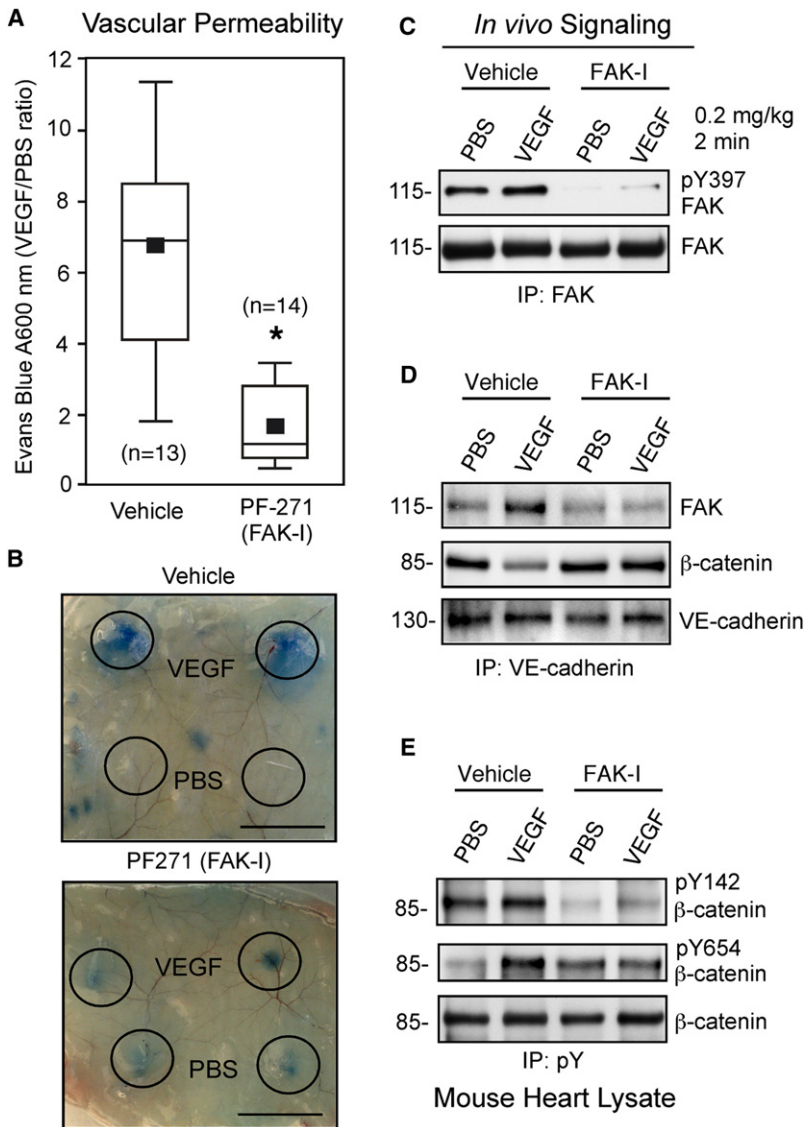


Figure 3. Pharmacological FAK Inhibition Prevents VEGF-Initiated VP and FAK Modulation of VE-Cadherin- β -Catenin Complex Formation and Phosphorylation In Vivo

(A) Quantification of dermal VP after VEGF (400 ng) or PBS injection (two sites each per mouse) with or without pretreatment with FAK inhibitor (PF271, 30 mg/kg). Evan's Blue dye leakage is plotted as a VEGF/PBS ratio. Box-whisker plots show the distribution of the data: black square, mean; bottom line, 25th percentile; middle line, median; top line, 75th percentile; and whiskers, 5th and 95th percentiles ($*p < 0.05$).

(B) Representative images of dye leakage. VEGF or PBS injection sites are circled. Scale bar represents 0.5 cm.

(C–E) Hearts of vehicle or FAK inhibitor (FAK-I) pretreated mice were analyzed 2 min after VEGF (0.2 mg/kg) or PBS tail vein injections by IP and immunoblotting. (C) FAK-I blocks FAK Y397 phosphorylation but not FAK expression. (D) VEGF-stimulated FAK/VE-cadherin association and VE-cadherin/ β -catenin dissociation is prevented by FAK-I administration as determined by co-IP analyses. (E) FAK-I treated mice exhibit loss of β -catenin Y142 phosphorylation by anti-pY IP analyses. Increased basal but prevention of VEGF-stimulated β -catenin Y654 phosphorylation by FAK-I. See also Figure S3.

β -catenin dissociation in FAK-WT but not FAK-KD mice (Figure 2E). FAK-KD mice showed reduced basal and VEGF-stimulated levels of β -catenin Y142 phosphorylation (Figure 2F). In contrast, FAK-KD mice showed normal basal levels of β -catenin phosphorylation on Y654 but this did not increase in response to VEGF as detected in FAK-WT mice (Figure 2F).

To assess β -catenin as a putative FAK substrate, in vitro kinase assays showed that recombinant FAK could readily phosphorylate β -catenin from human umbilical cord endothelial cells (HUVECs) and recombinant β -catenin was equally phosphorylated by FAK or Src (Figures S3A and S3B). Mass spectrometry analyses revealed that FAK phosphorylated

β -catenin at Y142 whereas Src phosphorylated β -catenin at Y654 (Figures S3C and S3D). Previous studies established that phosphorylation of β -catenin leads to disruption of cell adhesion: phosphorylation at Y142 disrupts α -catenin binding (Piedra et al., 2003) and phosphorylation at Y654 disrupts E-cadherin binding (Roura et al., 1999). Our results support the hypothesis that VEGF-stimulated FAK activation triggers FAK recruitment to a VE-cadherin complex whereby FAK phosphorylation of β -catenin at Y142 enhances junctional disassembly and VP.

were inhibited by FAK-KD expression in ECs (Figure S2B). Additionally, VEGF promoted elevated FAK Y861 phosphorylation in both FAK-WT and FAK-KD mice (Figures S2B–S2E). FAK Y397 is an autophosphorylation site, FAK Y576 is within the kinase domain activation loop, and FAK Y861 is in the C-terminal domain and a substrate for Src and other PTKs. Together, these results show that the FAK-KD mutation selectively prevents FAK activation within ECs associated with the inhibition of FAK Y397 and FAK Y576 but not FAK Y861 phosphorylation.

FAK-KD Blocks VEGF-Stimulated Regulation of AJ Proteins In Vivo

VEGF-induced VP results in part by rapid tyrosine phosphorylation of AJ proteins triggering disassembly (Dejana et al., 2008), but a direct role for FAK in this process has not been appreciated. We find that VEGF promoted a FAK/VE-cadherin complex as detected in FAK-WT but not FAK-KD in mouse heart lysates (Figure 2D). Correspondingly, VEGF triggered VE-cadherin/

Small Molecule FAK Inhibition Prevents VEGF-Initiated VP In Vivo

Although pharmacological FAK inhibition is linked to the prevention of VEGF-stimulated angiogenesis (Weis et al., 2008), alterations in VP precede angiogenesis. Pretreatment of mice with a small molecule FAK inhibitor (FAK-I) PF-262,271 (Roberts et al., 2008) significantly prevented ($p < 0.05$) VEGF-induced dermal VP compared to vehicle control (Figures 3A and 3B). In

analyzing heart lysates after tail vein injection of VEGF, FAK-I blocked FAK Y397 phosphorylation (Figure 3C), FAK/VE-cadherin association, β -catenin dissociation from VE-cadherin (Figure 3D), and Y142 β -catenin phosphorylation (Figure 3E). Mice treated with FAK-I showed increased basal β -catenin Y654 phosphorylation, but this did not change upon VEGF addition (Figure 3E). Taken together, both genetic and pharmacological results support the importance of FAK activity in the regulation of VP and β -catenin Y142 phosphorylation in mice.

FAK Inhibition Prevents VEGF-Induced Permeability In Vitro

Human pulmonary aortic endothelial cells (HPAECs) and HUVECs grown on Boyden chamber tissue culture inserts will form a tight cell monolayer that blocks the passage of macromolecules. VEGF-induced HUVEC permeability to high molecular weight dextran was prevented by FAK-I in a dose-dependent manner (Figure S4, $p < 0.001$) and FAK-I prevented VEGF-induced HPAEC paracellular permeability to IgG within 5 and 15 min (Figure 4A, $p < 0.001$). Notably, FAK-I also increased basal barrier strengthening within 15 to 30 min (Figure 4A, $p < 0.05$). These differences in basal and VEGF-stimulated permeability were verified by electrical resistance measurements of HPAECs (Figure 4B). Biochemically, FAK-I addition did not affect VEGF-induced VEGF-R2 or Src PTK activation under conditions where FAK Y397 phosphorylation was inhibited (Figure 4C). Staining of HUVECs for VE-cadherin revealed gaps in the cell monolayer after 60 min with VEGF that was prevented in the presence of FAK-I (Figure 4D).

Consistent with our findings in FAK-KD mouse hearts (Figures 2 and 3), pretreating HUVECs with FAK-I prevented VEGF-induced FAK/VE-cadherin association, blocked β -catenin Y142 phosphorylation, and inhibited VEGF-induced β -catenin Y654 phosphorylation (Figure 4E). FAK-I prevented VE-cadherin/ β -catenin dissociation upon VEGF addition to confluent HUVECs (Figure 4F) consistent with the inhibition of paracellular permeability. VEGF is also known to trigger the formation of integrin-associated focal adhesions and increased cellular tension in coordination with the disassembly of AJs in culture (Abedi and Zachary, 1997). Increased paxillin tyrosine phosphorylation is a marker of focal adhesion formation and VEGF effects on paxillin phosphorylation were blocked by FAK-I addition (Figure 4F). Treatment of cells with the myosin IIA inhibitor blebbistatin prevents cellular tension generation, limits focal adhesion formation, and prevents paxillin tyrosine phosphorylation (Pasapera et al., 2010). Interestingly, blebbistatin did not affect VEGF-stimulated FAK/VE-cadherin association or increased FAK Y397 phosphorylation under conditions where blebbistatin prevented VEGF-induced paxillin tyrosine phosphorylation (Figure 4G). These findings show that FAK activation and VE-cadherin association are separable from VEGF-initiated cytoskeletal tension-mediated changes in ECs.

FAK-KD ECs Establish a Barrier but Lack a Permeability Response to VEGF

Establishment of FAK null ECs is problematic due to growth and apoptosis defects in culture (Zhao et al., 2010). To study the role of FAK activity in EC barrier function in vitro, primary heart and lung ECs were isolated from 4- to 6-week-old mice and treated

with lentiviral Cre to create hemizygous FAK-WT and FAK-KD ECs (Figure S5A). These cells exhibited rapid uptake of acetylated low-density lipoprotein (Figure S5B) and showed equal surface expression of EC markers CD31 and ICAM-2 (Figure S5C). There was no overt difference in actin organization or VE-cadherin distribution at cell-cell junctions between FAK-WT and FAK-KD ECs (Figure S5D). Thus, in contrast to problems associated with FAK null ECs, FAK-KD expression allows for the growth of ECs in culture.

Although both FAK-WT and FAK-KD ECs grow to confluence and form a nonpermeable barrier to high molecular weight dextran, only FAK-WT ECs produced vascular leak in response to VEGF (Figure 5A). In FAK-KD ECs, FAK Y397 was inhibited despite normal VEGF-induced activation of VEGF-R2 and Src (Figure 5B). Inhibition of VEGF-initiated cell permeability in FAK-KD ECs was paralleled by the lack of VEGF-induced FAK/VE-cadherin association, VE-cadherin/ β -catenin dissociation, and β -catenin Y142 phosphorylation (Figure 5C). The transient association of FAK and VE-cadherin at 5 and 15 min after VEGF stimulation was prevented by FAK-I addition (Figure 5D). These results support an essential role for FAK activity downstream of VEGF-R2 and Src in the control of paracellular permeability.

Although transfection of cells with mutants of β -catenin can prevent epithelial junctional formation (Tominaga et al., 2008), the role of β -catenin tyrosine phosphorylation in regulating VE-cadherin association remains undetermined. VE-cadherin/ β -catenin association was equivalent in unstimulated HUVECs expressing His-tagged WT β -catenin versus Y142F or Y654F nonphosphorylatable β -catenin mutants (Figure 5E). VEGF stimulation disrupted the VE-cadherin/ β -catenin complex in cells expressing WT β -catenin, but Y142F or Y654F β -catenin mutants remained associated with VE-cadherin (Figures 5E and 5F). These results support the importance of Y142 and Y654 β -catenin phosphorylation in destabilizing VE-cadherin binding to β -catenin in response to VEGF.

Rapid FAK Localization to AJs in Response to VEGF

VE-cadherin is a transmembrane protein localized to cell-cell junctions and internalized upon VEGF stimulation to allow breakdown of junctional contacts (Dejana et al., 2008). FAK is a cytoplasmic PTK with an intracellular distribution influenced by integrin and growth factor receptor signals (Mitra et al., 2005). In confluent and quiescent HUVEC monolayers, FAK exhibits a cytoplasmic, nuclear, and adhesion site distribution as determined by confocal microscopy (Figure 6A). FAK staining did not detectably overlap with VE-cadherin at cell-cell junctions in quiescent HUVECs. However, VEGF stimulation triggers increased FAK accumulation at cell-cell junctions within 5 min that overlaps with VE-cadherin (Figure 6B). Real time imaging of a green fluorescent protein (GFP) fusion with FAK (GFP-FAK) revealed rapid accumulation at cell-cell contact sites within 30 to 60 s after VEGF addition (Figure 6C). Together, these analyses show that VEGF triggers FAK localization to cell-cell contacts and binding to VE-cadherin in the regulation of junctional stability.

Conformation-Regulated Binding of FAK to VE-Cadherin

The molecular mechanisms controlling FAK activation are intricate and involve the release of inhibitory intramolecular FAK

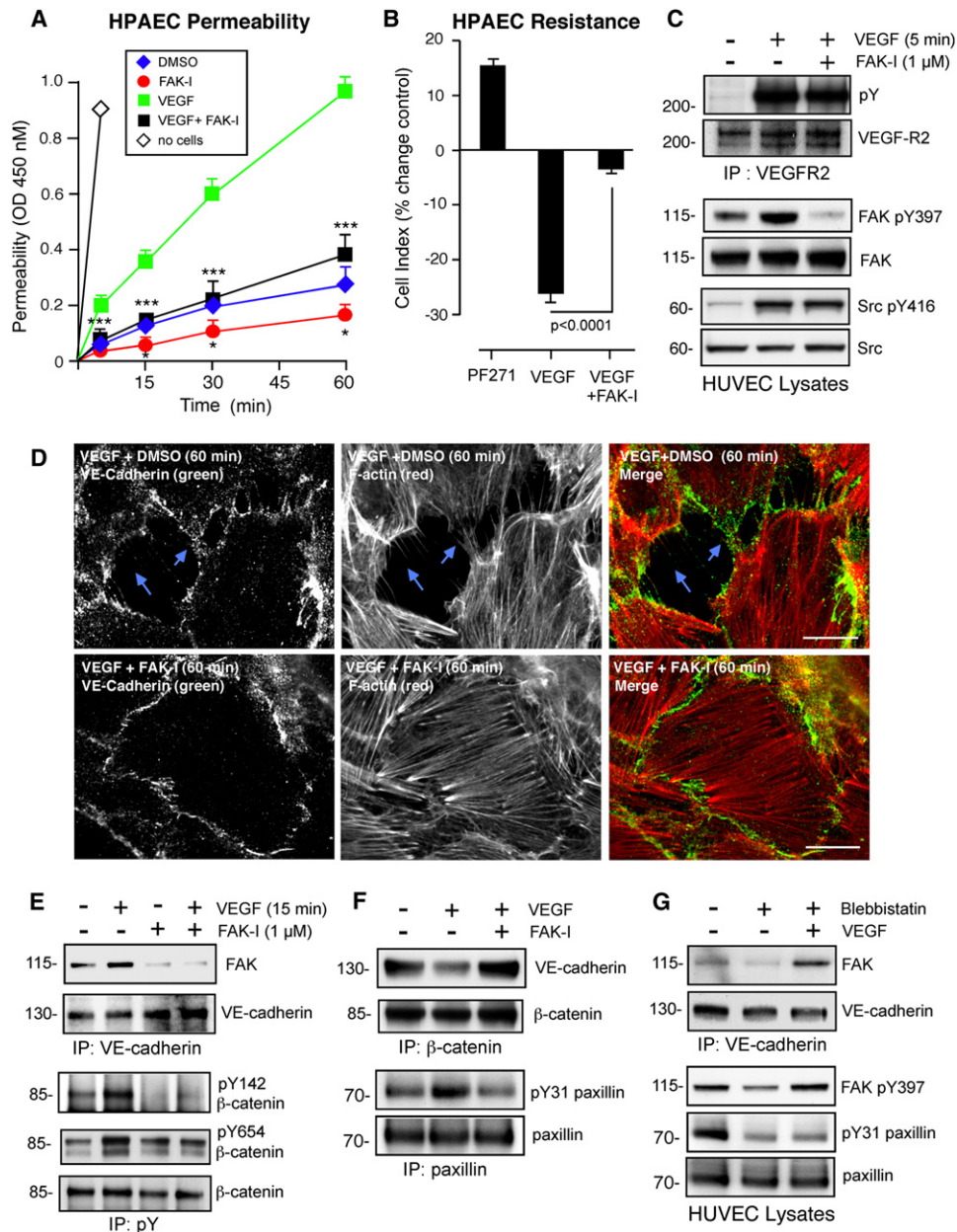


Figure 4. VEGF-Stimulated Paracellular Permeability and Adherens Junction Regulation Are Prevented by Pharmacological FAK-I Addition to Human ECs

(A) Time course (5–60 min) of VEGF-increased human pulmonary artery endothelial cells (HPAEC) permeability to HRP-conjugated IgG. Inhibition of basal ($p < 0.05$) and VEGF-stimulated ($***p < 0.001$) permeability by $1 \mu\text{M}$ PF271 (FAK-I) addition. Data is the mean \pm SD of 12 experimental points from two independent experiments.

(B) Significant inhibition of VEGF-stimulated change in HPAEC cell index (cell monolayer electrical resistance) at 90 min by $1 \mu\text{M}$ FAK-I addition ($p < 0.0001$) as measured by the Roche xCELLigence system. Values are normalized to DMSO controls and are means \pm SD from four independent Xcelligence chambers.

(C) FAK-I blocks FAK (pY397) but not Src (pY416) or VEGF-R2 tyrosine phosphorylation after VEGF addition (50 ng/ml, 5 min) of human umbilical vein endothelial cells (HUVEC) lysates.

(D) VEGF (50 ng/ml, 60 min) addition promotes cellular gaps (arrows) in a HUVEC monolayer that is prevented by FAK-I ($1 \mu\text{M}$) addition. Shown is anti-VE-cadherin (green) and actin (phalloidin, red) staining. Scale bar represents $10 \mu\text{m}$.

(E) FAK/VE-cadherin association, β -catenin Y142 phosphorylation, but not β -catenin Y654 phosphorylation is blocked by FAK-I addition to HUVECs.

(F) FAK-I prevents VEGF-stimulated VE-cadherin/ β -catenin complex dissociation and increased paxillin phosphorylation by IP and immunoblotting analyses.

(G) VEGF-stimulated FAK/VE-cadherin binding and increased FAK Y397 but not paxillin Y31 tyrosine phosphorylation occurs in the presence of the nonmuscle myosin IIA inhibitor blebbistatin ($20 \mu\text{M}$). See also Figure S4.

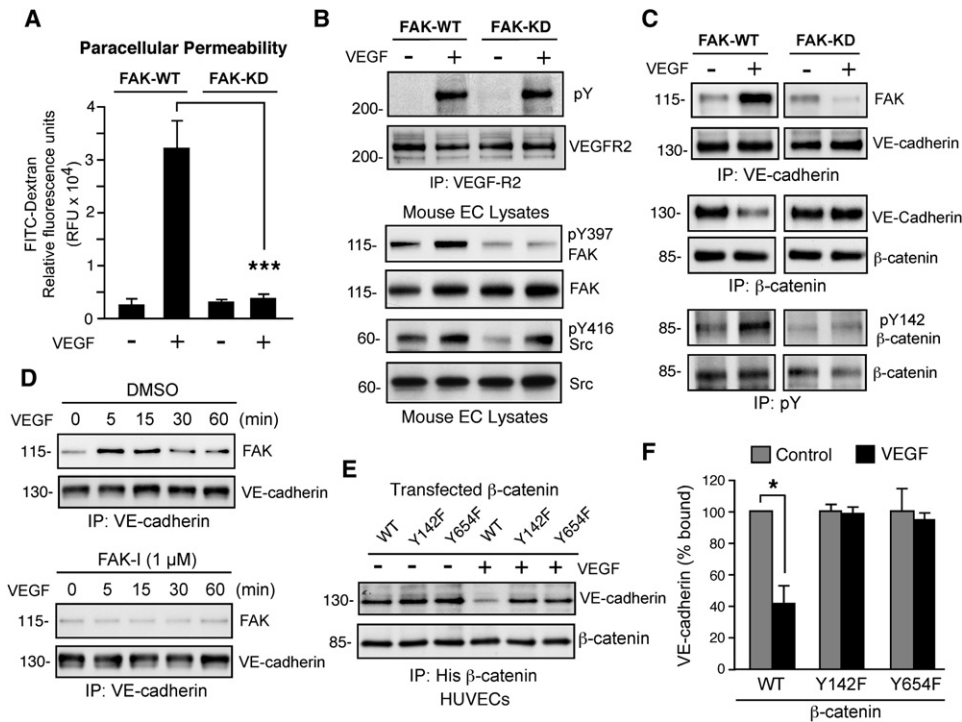


Figure 5. Genetic Inhibition of FAK Prevents VEGF-Stimulated Permeability Independent of Src

(A) FAK-KD ECs establish a barrier to FITC-dextran but lack a permeability response to VEGF. Values are means ± SD from one of two independent experiments (***p* < 0.001).

(B) No differences in VEGF-R2, Pyk2 Y402, and Src Y416 tyrosine phosphorylation upon VEGF (50 ng/ml, 15 min) addition to FAK-WT and FAK-KD ECs by IP and immunoblotting analyses. FAK-WT but not FAK-KD phosphorylation at Y397 after VEGF addition.

(C) FAK-KD mutation prevents FAK/VE-cadherin association, VE-cadherin/β-catenin dissociation, and β-catenin Y142 phosphorylation after VEGF stimulation.

(D) FAK-I prevents VEGF-stimulated FAK/VE-cadherin association by co-IP analyses.

(E) Mutation of β-catenin Y142 prevents VE-cadherin dissociation after VEGF stimulation. β-catenin constructs were transfected into HUVECs and VE-cadherin association determined by co-IP analyses.

(F) Percent of VE-cadherin association with His-tagged β-catenin as determined by densitometry. Values are means ± SD from two samples (*p* < 0.05). See also Figure S5.

FERM domain contacts with the FAK kinase region (Frame et al., 2010). Structural studies show that FAK FERM domain mutations (Y180A, M183A) can prevent this restraint, resulting in constitutively-active FAK (Lietha et al., 2007). These mutations were introduced into GFP-FAK-WT and GFP-FAK-KD and analyzed for effects on VE-cadherin binding in HUVECs (Figure 7A). As expected, VEGF promoted FAK-WT but not FAK-KD association with VE-cadherin. FAK FERM domain mutations (Y180A, M183A) in FAK-WT resulted in increased FAK Y397 phosphorylation and VEGF-independent association with VE-cadherin (Figure 7A). Notably, the same FAK FERM domain mutations in FAK-KD did not enhance FAK Y397 phosphorylation but resulted in VEGF-independent FAK-KD/VE-cadherin association (Figure 7A). These results support the notion that FAK is conformationally-activated in response to VEGF and that FAK-KD is locked in a closed conformation that prevents VE-cadherin association.

The FAK FERM Domain Binds to VE-Cadherin and Localizes to Cell-Cell Contacts

Since VEGF stimulation of ECs promotes rapid FAK accumulation at cell-cell contacts and association with VE-cadherin,

analyses were performed to determine if this represents a direct binding interaction. In vitro translation of various FAK constructs combined with pull-down assays using a glutathione-S-transferase fusion protein encompassing the VE-cadherin cytoplasmic domain (621–784), revealed direct binding of FAK-WT, FAK-FERM, but not the FAK C-terminal domain to VE-cadherin (Figure 7B). Additionally, GFP-FAK FERM expression in HUVECs formed a VEGF-independent complex with VE-cadherin (Figure 7C) and FAK-FERM was distributed in the cell nucleus (Lim et al., 2008) as well as colocalized with VE-cadherin at cell-cell junctions (Figure 7D). Together, these results support the conclusion that VEGF stimulation of cells activates FAK in a conformational manner triggering FAK FERM binding to VE-cadherin at cell-cell junctions where FAK phosphorylates β-catenin at Y142 to promote junctional disassembly in vitro and vascular permeability in vivo.

DISCUSSION

During development, there is a complex interplay between receptors for angiogenic growth factors, integrins, and cadherins in the processes of vasculogenesis and angiogenesis (Hynes,

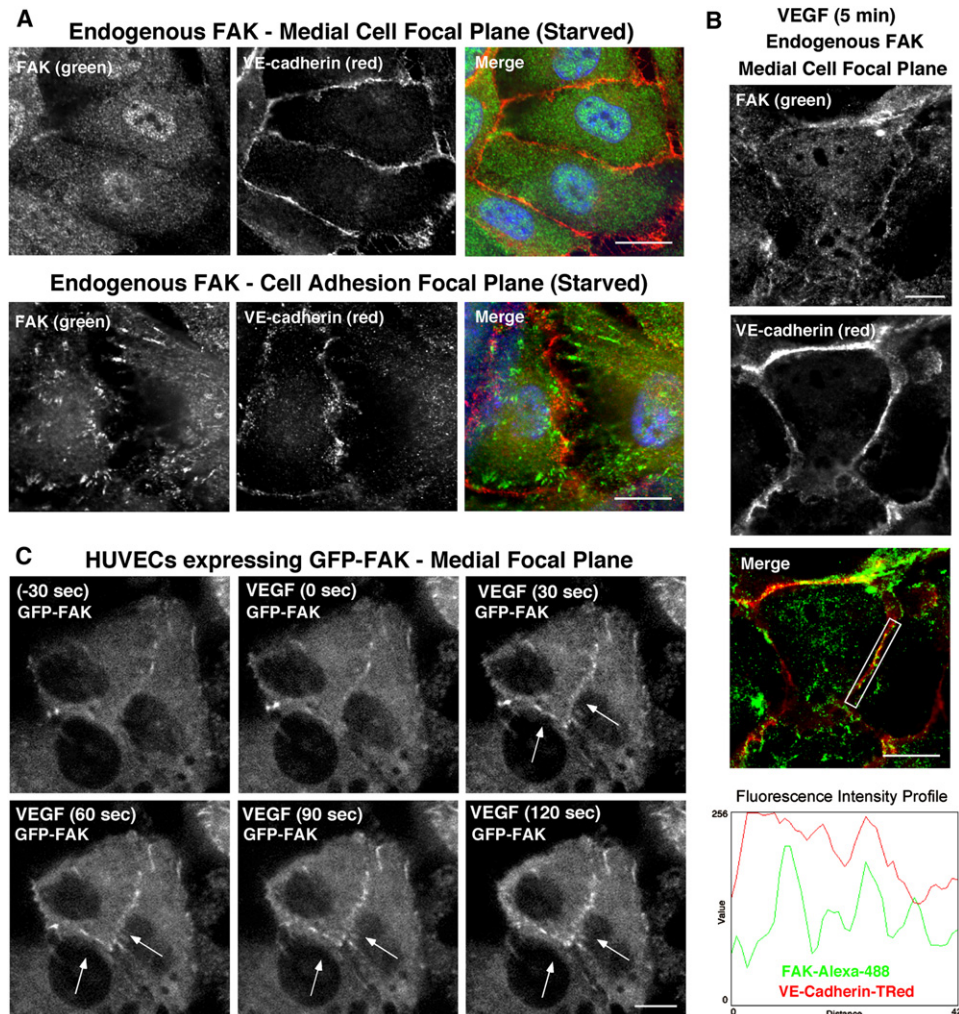


Figure 6. VEGF-Stimulated Recruitment of FAK to EC Adherens Junctions

(A) Staining for endogenous FAK (green) reveals nuclear, cytoplasmic, and focal adhesion distribution within starved HUVECs without overlap with VE-cadherin (red) at cell-cell junctions. Scale bar represents 10 μm .

(B) VEGF (50 ng/ml, 5 min) promotes FAK (green) and VE-cadherin (red) colocalization in HUVECs at cell-cell junctions (yellow, merge). Scale bar represents 10 μm . Fluorescence intensity profiles of the indicated boxed region were obtained using ImageJ (v1.43).

(C) Live-cell confocal microscopy (medial focal plane) reveals rapid VEGF-stimulated GFP-FAK accumulation (arrows) at HUVEC cell-cell junctions. Image montage (–30 to 120 s) before and after VEGF (50 ng/ml) addition. Scale bar represents 10 μm .

2007). FAK is activated by both growth factors and integrins and functions as a signaling nexus between these pathways. FAK knockout (Ilic et al., 2003) or FAK-KD knockin prevent functional blood vessel formation (Lim et al., 2010a; Zhao et al., 2010). Because FAK null ECs exhibit increased apoptosis (Braren et al., 2006; Ilic et al., 2003; Shen et al., 2005) and FAK loss triggers compensatory Pyk2 PTK expression (Lim et al., 2010b; Weis et al., 2008), it has been difficult to validate and confirm FAK-specific signaling connections that are relevant in vivo.

Here, we have overcome the FAK-KD embryonic lethal phenotype by creating an inducible mouse model resulting in hemizygous WT or FAK-KD expression in ECs. Blocking FAK activity in ECs prevented VEGF-stimulated vascular permeability without gross alterations in vessel structure or barrier establishment in vitro. We identified β -catenin Y142 as a substrate for FAK

and showed that VEGF-stimulated FAK activation promotes FAK FERM-mediated binding to VE-cadherin at cell-cell junctions, β -catenin Y142 phosphorylation, VE-cadherin/ β -catenin dissociation, and EC junctional breakdown associated with increased paracellular permeability. We show via mutagenesis that FAK FERM domain intramolecular restraints prevent FAK-KD and VE-cadherin association in cells. Although the VEGF-initiated signal that promotes FAK conformational activation remains unknown, our results support a model as first proposed by Frame et al. (2010) whereby FAK FERM interactions function to promote FAK recruitment to a specific signaling complex (adherens junctions) and maintenance of an activated FAK state by FERM-partner (VE-cadherin) binding. In addition to directly connecting FAK to the control of adherens junction dynamics, our findings also support the emerging importance of FAK FERM

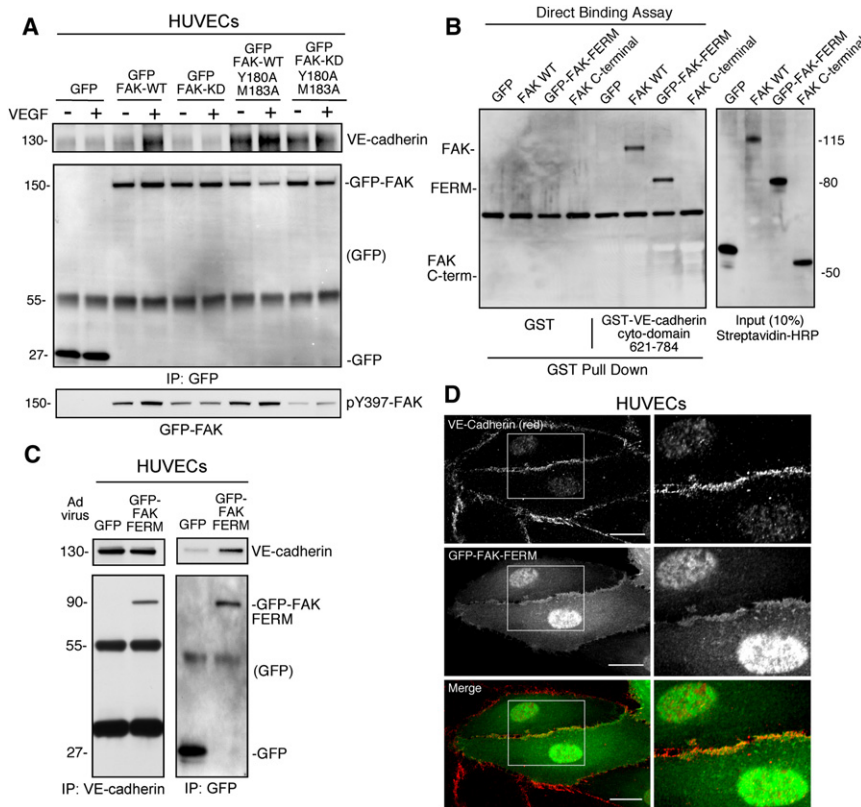


Figure 7. FAK FERM Mutations Release Conformational Restraint in FAK and Allow for Direct FAK FERM Binding to VE-Cadherin Cytoplasmic Domain

(A) FAK FERM F2 lobe mutations (Y180A, M183A) promote VEGF-independent association of both FAK-WT and FAK-KD with VE-cadherin. The indicated GFP-FAK constructs were transfected in HUVECs and associations determined by co-IP analyses in starved or VEGF-stimulated cells. FAK FERM Y180/183A mutations do not promote phosphorylation of FAK-KD at Y397.

(B) FAK FERM binds directly to VE-cadherin. In vitro translated GFP, FAK-WT, FAK-KD, GFP-FAK FERM, and FAK C-terminal domain were used in a direct binding assay with glutathione-S-transferase (GST) or GST-fusions of the VE-cadherin cytoplasmic domain (621–784). Streptavidin-HRP analyses show the amount of FAK bound (left) or 10% of input (right). GFP and GFP-FAK FERM contain a tandem affinity probe tag.

(C) GFP-FAK FERM (1–402) associates with endogenous VE-cadherin. Co-IP analyses were performed using antibodies to GFP or VE-cadherin in adenovirus (Ad) infected HUVECs.

(D) FAK FERM localizes to adherens junctions and to the nucleus in HUVECs. Cells were analyzed for VE-cadherin (red) and GFP-FAK-FERM (green) and the merged image is shown. Inset, enlarged area (boxed) shows colocalization at cell-cell junctions (yellow) in the merged image. TO-PRO-3 iodide (642/661) was used as a nuclear marker. Scale bar represents 10 μm.

domain linkages in growth factor receptor signaling pathways (Chen et al., 2011; Plaza-Menacho et al., 2011).

Another notably finding was that alterations in adherens junction tyrosine phosphorylation by genetic or pharmacological FAK inhibition occurred downstream of VEGF receptor or Src PTK activation in vivo and in vitro. FAK inhibition prevented β -catenin Y142 phosphorylation and also blocked VEGF-stimulated β -catenin Y654 phosphorylation. In vitro, β -catenin Y142 was phosphorylated by FAK whereas Y654 was phosphorylated by Src. β -catenin expression is required for EC junctional formation and forms a linkage between VE-cadherin and the actin cytoskeleton (Cattelino et al., 2003). Phosphorylation of β -catenin at Y142 disrupts α -catenin binding and connections to actin whereas β -catenin Y654 phosphorylation regulates binding to cadherins (Lilien and Balsamo, 2005; Roura et al., 1999). We found that Y142F or Y654F β -catenin mutations prevent VEGF-stimulated β -catenin dissociation from VE-cadherin consistent with multiple phosphorylation site control of adherens junction stability. Moreover, we speculate that loss of FAK catalytic activity and corresponding inhibition of FAK Y397 phosphorylation may prevent the formation of a FAK-Src signaling complex important in regulating cadherin internalization (Canel et al., 2010). It is possible that the rapid relocalization of FAK to cell-cell junctions in response to VEGF, coinciding with FAK Y397 auto-phosphorylation, may serve as a platform for Src recruitment. As small molecule inhibitor and mouse knockout studies support Src PTK importance in VEGF-mediated regulation of adherens junction tyrosine phosphorylation (Weis and Cheresh, 2005), it is likely

that combined or sequential actions of FAK and Src act to control vascular permeability.

Changes in vascular permeability often precede or accompany tumor progression (Weis and Cheresh, 2005). Notably, activated FAK is localized to sites of vascular hyper-permeability (Hiratsuka et al., 2011) and loss of EC-associated FAK expression inhibits glioma-associated permeability of the blood-brain barrier (Lee et al., 2010). Previous studies support the importance of FAK activity in the regulation of Rho-family GTPase-associated contractile cell changes needed for barrier permeability and re-strengthening (Quadri, 2011; Thennes and Mehta, 2011). To this end, pharmacological FAK inhibition prevents VEGF-stimulated paxillin tyrosine phosphorylation, a marker of focal adhesion formation. However, inhibition of myosin-mediated cell contractility did not affect VEGF-induced FAK association with VE-cadherin and increased Y397 FAK phosphorylation but did prevent VEGF-associated paxillin tyrosine phosphorylation. Thus, our findings point to distinct roles for FAK activity in the control of adherens junction tyrosine phosphorylation and cell contractility, both of which are important in the regulation of vascular permeability.

In summary, we show that VEGF promotes tension-independent FAK activation, rapid FAK localization to cell-cell junctions, binding of the FAK FERM domain to VE-cadherin, and direct FAK phosphorylation of β -catenin Y142 associated with VE-cadherin/ β -catenin dissociation and EC junctional breakdown. As genetic or pharmacological FAK inhibition prevents VEGF-stimulated vascular permeability, these studies establish the importance of FAK activity in adherens junction

regulation and support the use of FAK inhibitors in the treatment of vascular disease.

EXPERIMENTAL PROCEDURES

Mice

Floxed FAK mice (FAK^{fl/fl}) with two loxP sites flanking exon 3 of the FAK gene (Shen et al., 2005) and containing tamoxifen-inducible Cre-ER(T) driven by the 5' endothelial enhancer of the stem cell leukemia locus (Weis et al., 2008) were crossed with heterozygous mice containing a FAK KD mutation within exon 18 (FAK^{KD/WT}) (Lim et al., 2010a). FAK^{fl/KD}, FAK^{fl/WT}, FAK^{fl/KD} Cre-ER(T), and FAK^{fl/WT} Cre-ER(T) progeny were identified by genotyping using PCR as described (Lim et al., 2010a; Weis et al., 2008). FAK^{fl/fl} Cre-ER(T) mice were bred onto a Cre reporter strain (B6.129S4-Gt(ROSA)26Sortm1Sor/J) that contains a loxP-flanked DNA stop sequence preventing LacZ expression (Jackson Laboratory) to verify the efficacy of tamoxifen-induced Cre. Age-matched littermates were used for all experiments. At 6 weeks of age, FAK^{fl/KD} Cre-ER(T) and FAK^{fl/WT} Cre-ER(T) mice were treated with 2 mg tamoxifen (Sigma) every 2 days (intraperitoneal injection in corn oil) for 2 weeks to induce EC-specific Cre expression and FAK deletion. Mice were used for experiments at 10 weeks of age. The UCSD Institutional Animal Care and Use Committee approved all mouse procedures.

Antibodies and Reagents

Antibodies to Src, VEGF-R2, β -catenin, and phosphospecific β -catenin pY654 were from Santa Cruz Biotechnology. FAK and phosphotyrosine antibodies were from Millipore. Antibodies to Pyk2, paxillin, CD31, VE-cadherin, and ICAM-2 were from BD Biosciences. Phosphospecific antibodies (FAK Y397, FAK Y576, FAK Y861, and Pyk2 Y402) and antibodies to β -galactosidase were from Life Technologies. Phosphospecific antibodies to Src Y416, β -catenin Y142, and paxillin Y31 were from Cell Signaling Technology, Abcam, and BioSource, respectively. Antibodies to GFP and to His-tag were from Covance and QIAGEN. Human VEGF-165 was from Peprotech. PF-262,271 FAK inhibitor (FAK-I) was synthesized as described (Roberts et al., 2008). Blebbistatin was from Enzo Life Sciences. GFP-FAK expressing HUVECs and adenoviral GFP-FAK FERM (1-402) were created as described (Lim et al., 2008). GST-VE cadherin (621-784) was generated via PCR and cloned into pGEX4T1 vector for bacterial expression. The GFP fragment from pEGFPC1 was cloned into pCDNA3.1/hygro TAP (tandem affinity purification) to create GFP-TAP tag. pEGFP-C1 FAK Y180A/M138A and pEGFP-C1 FAK-KD Y180A/M138A were created by mutagenesis (QuickChange XL, Agilent Technologies). All constructs were verified by DNA sequencing.

Vascular Studies

Mice were intravenously injected with Alexa flour 568-labeled GSLI/BSLI (endothelial specific) lectin (Invitrogen, 20 μ g/mouse). After 15 min, mouse tissues (heart and diaphragm) were dissected, and whole mounts analyzed by laser scanning confocal microscopy (Nikon C1si, PlanApo 20 \times N.A. 0.75). A modified Miles assay was used to evaluate VEGF-induced Evan's blue dye leak in the skin as described (Eliceiri et al., 1999). Two injection sites of recombinant VEGF (400 ng) or PBS were analyzed per mouse. FAK-I (30 mg/kg) solubilized in 30% 2-hydroxypropyl- β -cyclodextrin and 2.5% dextrose was administered twice-daily (BID) via oral gavage 36 hr prior to initiation of Miles dermal vessel permeability or heart-associated signaling assays.

Signaling

Tamoxifen-treated FAK^{fl/KD} Cre-ER(T) and FAK^{fl/WT} Cre-ER(T) mice were tail vein injected with VEGF (0.2 mg/kg in 100 μ l PBS) or PBS alone and after 2 min, hearts were rapidly excised and either homogenized for protein lysates (Weis et al., 2004b) or embedded in optimal cutting temperature (OCT, Tissue Tech) compound and quickly frozen. Confluent HUVECs or mouse ECs were starved for 6 hr in basal medium, and DMSO or FAK-I were added 1 hr prior to VEGF addition (50 ng/ml). Transfections were performed with indicated plasmids using JetPEI for HUVECs (Polyplus Transfection). Total protein lysates were prepared in Extraction Buffer containing 50 mM HEPES, pH 7.4, 150 mM NaCl, 1% Triton X-100, 1% sodium deoxycholate, 0.1% SDS, 10% glycerol, and protease inhibitors. For immunoprecipitation and GST binding analyses, lysates were diluted 2-fold in HNTG buffer (50 mM

HEPES, pH 7.4, 150 mM NaCl, 0.1% Triton, 10% glycerol), incubated with antibodies (1 μ g) or glutathione-agarose beads (Sigma) for 3 hr at 4°C, antibodies collected with either Protein A or G Plus (Millipore) agarose beads, and beads washed at 4°C in 1% Triton-only Extraction Buffer, followed by washes with HNTG buffer, and resolved by SDS-PAGE. Sequential immunoblotting analyses were performed as described (Lim et al., 2010a).

Tissue and Cell Staining

For X-gal staining, hearts were fixed in 0.25% glutaraldehyde and 2% paraformaldehyde in wash buffer (PBS with 2 mM MgCl₂) for 60 min on ice. After washing, hearts were incubated overnight at 37°C in PBS with 5 mM potassium ferrocyanide, 5 mM potassium ferricyanide, and 1 mg/mL 5-bromo-4-chloro-3-indolyl- β -D-galactopyranoside. Frozen heart sections in OCT were prepared (6 μ m, Leica CM1950), fixed in cold acetone (10 min), rehydrated in PBS containing 0.5% BSA (5 min), and blocked with 1.25% normal goat serum in PBS (30 min at RT). Samples were incubated with anti-FAK pY576 (1:50), anti-FAK pY861 (1:50), anti- β -galactosidase (1:2,000), and anti-CD31 (1:300) overnight at 4°C followed by Alexa Fluor-488 rat and Alexa Fluor-594 secondary antibodies (Invitrogen 1:500, 30 min at RT). pY861 blocking peptide was from Santa Cruz Biotechnology.

For cell staining, ECs were grown to confluency on 0.1% gelatin coated glass coverslips, fixed in 3.7% paraformaldehyde (15 min at RT), permeabilized with 0.1% Triton X-100 (3 min), incubated with anti-VE-cadherin (1:25) or anti-FAK antibodies (1:50), followed by Alexa Fluor-488 or rhodamine-labeled goat anti-mouse secondary antibodies (Jackson). Texas Red phalloidin (Invitrogen) and Hoechst 33342 (10 μ g/ml, Invitrogen) were used visualize actin and cell nuclei, respectively. Confluent and starved GFP-FAK expressing HUVECs on glass bottom dishes (MatTek) were imaged every 10 s in a humidified, 5% CO₂ environment at 37°C prior to and immediately after 50 ng/ml VEGF addition. Imaging was performed using an Olympus IX81 spinning disk confocal microscope with zero drift compensation focus control, 60 \times PlanApo (N.A. 1.42), and Hamamatsu OrcaER camera controlled by Slidebook software. Files were cropped, pseudo-colored, and contrast-adjusted using Adobe Photoshop. Degree of association exhibited by patterns of fluorescence was measured on a pixel-by-pixel basis and calculated as a Pearson's correlation coefficient using the "measure correlations" module (Cell Profiler, v2.0, Broad Institute). A value of 0 indicates no overlap and a value of 1 corresponds to 100% colocalization.

Paracellular Permeability

Cells (1 \times 10⁵) were plated in Transwell chambers (Costar; 6.5 mm diameter, 0.4 μ m pore size), grown for 3 days, and serum starved for 4 hr. HRP-conjugated IgG (4 μ g/ml) and VEGF (100 ng/ml) were added to the upper chamber. At 0, 5, 15, 30, and 60 min, 10 μ l of media was removed from the lower chamber and the amount of horseradish peroxidase-conjugated IgG determined by ELISA (Ultra TMB, Thermo) and 450 nm fluorescence measured by a plate reader (TECAN). Transwell assays were also performed with FITC-labeled dextran (2 million daltons). Control cells received serum and no VEGF. Maximum values were determined without cells. Where indicated, FAK-I was added to the upper chamber 1 hr prior to VEGF. For xCELLigence (Roche, RTCA DP Station) electrical conductivity assays, HPAECs were grown to confluence on gelatin-coated 16-well E-plates, starved for 2 hr prior to FAK inhibitor or VEGF addition, and values normalized to DMSO addition. Values represent the mean of triplicate points for all experiments.

β -Catenin Phosphorylation by FAK and Src

β -catenin was immunoprecipitated from starved HUVECs and incubated in kinase buffer (20 mM Tris HCl, pH 7.5, 200 mM NaCl, 0.5 mM Na₃VO₄, 25 mM MgCl₂, 5 mM MnCl₂, 1 mM EDTA, 5 mM β -mercaptoethanol, and 200 μ M ATP) in the presence or absence of recombinant FAK kinase domain (Wu et al., 2008) for 15 min at 32°C. Recombinant β -catenin (2 μ g, Abnova) was phosphorylated in vitro by addition of recombinant FAK kinase domain or full-length His-tagged Src as purified from baculovirus (Wu et al., 2008). β -catenin was eluted from poly-acrylamide gels, digested by trypsin and endoproteinase GluC, and peptides were analyzed by LC-MS/MS using a QSTAR-Elite hybrid mass spectrometer (Applied Biosystems). Peptide identifications were made using paragon algorithm executed in Protein Pilot 2.0 (Life Technologies) and MASCOT (Matrix Science) at the UCSD Core Proteomic facility.

EC Isolation and Culture

Primary mouse heart and lung ECs were isolated from 4- to 6-week-old mice. Early passage cells were immortalized by retroviral large T-antigen (Addgene) expression and puromycin selection. Lentiviral Cre recombinase (Allele Biotech) was used to inactivate floxed FAK as described (Lim et al., 2010b). For floxed exon 3, a 1.5 Kb PCR product is WT, 1.6 KB is floxed, and Cre deletion results in a 550 bp PCR product. For exon 18 within the FAK kinase domain, a 550 bp PCR product is WT and 550 plus 600 bp products denote FAK KD. EC phenotype was verified by 1,1'-dioctadecyl-3,3',3'-tetramethylindocarbocyanine perchlorate-acetylated-low density lipoprotein (Dil-Ac-LDL) uptake (10 µg/ml, for 4 hr) and evaluated for fluorescence. CD31 and ICAM-2 flow cytometry were performed using FITC-conjugated rat anti-mouse CD31 (1:100) and biotinylated rat anti-mouse ICAM-2 (1:100). APC-conjugated streptavidin (1:100, Invitrogen) was used to detect biotinylated ICAM-2 antibody and cells were analyzed using a FACScalibur. HUVECs and HPAECs were from Lonza and propagated as described (Weis et al., 2008). Experiments used cells passage <8.

In Vitro Translation and Binding

FAK constructs (prey) in pCDNA3.1 (1 µg) were in vitro translated in the presence of biotin-lysine (TNT System, Promega) and diluted 50-fold into Binding Buffer (50 mM HEPES pH7.4, 150 mM NaCl, 1% Triton X-100). Bait protein GST or GST VE-cadherin (621–784) were expressed in bacteria, purified, pre-bound to glutathione-agarose beads, and 10 µg incubated with in vitro translated constructs for 2 hr at 4°C. Beads were washed three times in Binding Buffer, resolved by SDS-PAGE, transferred to PVDF membranes whereby the bait protein was detected by Coomassie staining and the bound prey detected by streptavidin-HRP immunoblotting.

Statistics

Differences between groups were determined using one-way ANOVA with Tukey post hoc. Differences between pairs of data were determined using an unpaired two-tailed Student's t test. Analyses were performed using GraphPad Prism (v5.0b).

SUPPLEMENTAL INFORMATION

Supplemental Information includes five figures and can be found with this article online at doi:10.1016/j.devcel.2011.11.002.

ACKNOWLEDGMENTS

We thank Addolorata Maria Luce Coluccia (University of Salento, Italy) for providing His-tagged β -catenin constructs. We appreciate the generosity of Roche Applied Science for use of the xCELLigence DP analyzer. This work was supported by NIH HL093156 to D.D.S. J.O.N. was supported by the National Research Foundation of Korea (NRF-2011-0013182). Postdoctoral fellowship support was provided by Canadian Institutes of Health Research to C.L. (200810MFE-193594-139144), American Heart Association to A.T. (0825166F), and Susan G. Komen for the Cure to I.T. (KG111237). J.L.G. was supported by NIH HL073394 and L.M.A. was supported by K01 CA148897.

Received: April 27, 2011

Revised: October 4, 2011

Accepted: November 7, 2011

Published online: January 17, 2012

REFERENCES

Abedi, H., and Zachary, I. (1997). Vascular endothelial growth factor stimulates tyrosine phosphorylation and recruitment to new focal adhesions of focal adhesion kinase and paxillin in endothelial cells. *J. Biol. Chem.* 272, 15442–15451.

Abu-Ghazaleh, R., Kabir, J., Jia, H., Lobo, M., and Zachary, I. (2001). Src mediates stimulation by vascular endothelial growth factor of the phosphorylation

of focal adhesion kinase at tyrosine 861, and migration and anti-apoptosis in endothelial cells. *Biochem. J.* 360, 255–264.

Adam, A.P., Sharenko, A.L., Pumiglia, K., and Vincent, P.A. (2010). Src-induced tyrosine phosphorylation of VE-cadherin is not sufficient to decrease barrier function of endothelial monolayers. *J. Biol. Chem.* 285, 7045–7055.

Avraham, H.K., Lee, T.H., Koh, Y., Kim, T.A., Jiang, S., Sussman, M., Samarel, A.M., and Avraham, S. (2003). Vascular endothelial growth factor regulates focal adhesion assembly in human brain microvascular endothelial cells through activation of the focal adhesion kinase and related adhesion focal tyrosine kinase. *J. Biol. Chem.* 278, 36661–36668.

Birukova, A.A., Cokic, I., Moldobaeva, N., and Birukov, K.G. (2009). Paxillin is involved in the differential regulation of endothelial barrier by HGF and VEGF. *Am. J. Respir. Cell Mol. Biol.* 40, 99–107.

Braren, R., Hu, H., Kim, Y.H., Beggs, H.E., Reichardt, L.F., and Wang, R. (2006). Endothelial FAK is essential for vascular network stability, cell survival, and lamellipodial formation. *J. Cell Biol.* 172, 151–162.

Canel, M., Serrels, A., Miller, D., Timpson, P., Serrels, B., Frame, M.C., and Brunton, V.G. (2010). Quantitative in vivo imaging of the effects of inhibiting integrin signaling via Src and FAK on cancer cell movement: effects on E-cadherin dynamics. *Cancer Res.* 70, 9413–9422.

Cattellino, A., Liebner, S., Gallini, R., Zanetti, A., Balconi, G., Corsi, A., Bianco, P., Wolburg, H., Moore, R., Oreda, B., et al. (2003). The conditional inactivation of the beta-catenin gene in endothelial cells causes a defective vascular pattern and increased vascular fragility. *J. Cell Biol.* 162, 1111–1122.

Chen, T.H., Chan, P.C., Chen, C.L., and Chen, H.C. (2011). Phosphorylation of focal adhesion kinase on tyrosine 194 by Met leads to its activation through relief of autoinhibition. *Oncogene* 30, 153–166.

Corsi, J.M., Houbron, C., Billuart, P., Brunet, I., Bouvrée, K., Eichmann, A., Girault, J.A., and Enslin, H. (2009). Autophosphorylation-independent and -dependent functions of focal adhesion kinase during development. *J. Biol. Chem.* 284, 34769–34776.

De, S., Razorenova, O., McCabe, N.P., O'Toole, T., Qin, J., and Byzova, T.V. (2005). VEGF-integrin interplay controls tumor growth and vascularization. *Proc. Natl. Acad. Sci. USA* 102, 7589–7594.

Dejana, E., Orsenigo, F., and Lampugnani, M.G. (2008). The role of adherens junctions and VE-cadherin in the control of vascular permeability. *J. Cell Sci.* 121, 2115–2122.

Dejana, E., Tournier-Lasserre, E., and Weinstein, B.M. (2009). The control of vascular integrity by endothelial cell junctions: molecular basis and pathological implications. *Dev. Cell* 16, 209–221.

Eliceiri, B.P., Paul, R., Schwartzberg, P.L., Hood, J.D., Leng, J., and Cheresh, D.A. (1999). Selective requirement for Src kinases during VEGF-induced angiogenesis and vascular permeability. *Mol. Cell* 4, 915–924.

Eliceiri, B.P., Puente, X.S., Hood, J.D., Stupack, D.G., Schlaepfer, D.D., Huang, X.Z., Sheppard, D., and Cheresh, D.A. (2002). Src-mediated coupling of focal adhesion kinase to integrin $\alpha(v)\beta_5$ in vascular endothelial growth factor signaling. *J. Cell Biol.* 157, 149–160.

Ferrara, N., Gerber, H.P., and LeCouter, J. (2003). The biology of VEGF and its receptors. *Nat. Med.* 9, 669–676.

Frame, M.C., Patel, H., Serrels, B., Lietha, D., and Eck, M.J. (2010). The FERM domain: organizing the structure and function of FAK. *Nat. Rev. Mol. Cell Biol.* 11, 802–814.

Harris, E.S., and Nelson, W.J. (2010). VE-cadherin: at the front, center, and sides of endothelial cell organization and function. *Curr. Opin. Cell Biol.* 22, 651–658.

Herzog, B., Pellet-Many, C., Britton, G., Hartzoulakis, B., and Zachary, I.C. (2011). VEGF binding to NRP1 is essential for VEGF stimulation of endothelial cell migration, complex formation between NRP1 and VEGFR2, and signaling via FAK Tyr407 phosphorylation. *Mol. Biol. Cell* 22, 2766–2776.

Hiratsuka, S., Goel, S., Kamoun, W.S., Maru, Y., Fukumura, D., Duda, D.G., and Jain, R.K. (2011). Endothelial focal adhesion kinase mediates cancer cell homing to discrete regions of the lungs via E-selectin up-regulation. *Proc. Natl. Acad. Sci. USA* 108, 3725–3730.

- Hynes, R.O. (2007). Cell-matrix adhesion in vascular development. *J. Thromb. Haemost.* 5 (Suppl 1), 32–40.
- Ilic, D., Kovacic, B., McDonagh, S., Jin, F., Baumbusch, C., Gardner, D.G., and Damsky, C.H. (2003). Focal adhesion kinase is required for blood vessel morphogenesis. *Circ. Res.* 92, 300–307.
- Lee, J., Borboa, A.K., Chun, H.B., Baird, A., and Eliceiri, B.P. (2010). Conditional deletion of the focal adhesion kinase FAK alters remodeling of the blood-brain barrier in glioma. *Cancer Res.* 70, 10131–10140.
- Liang, W., Kujawski, M., Wu, J., Lu, J., Herrmann, A., Loera, S., Yen, Y., Lee, F., Yu, H., Wen, W., and Jove, R. (2010). Antitumor activity of targeting SRC kinases in endothelial and myeloid cell compartments of the tumor microenvironment. *Clin. Cancer Res.* 16, 924–935.
- Lietha, D., Cai, X., Ceccarelli, D.F., Li, Y., Schaller, M.D., and Eck, M.J. (2007). Structural basis for the autoinhibition of focal adhesion kinase. *Cell* 129, 1177–1187.
- Lilien, J., and Balsamo, J. (2005). The regulation of cadherin-mediated adhesion by tyrosine phosphorylation/dephosphorylation of beta-catenin. *Curr. Opin. Cell Biol.* 17, 459–465.
- Lim, S.T., Chen, X.L., Lim, Y., Hanson, D.A., Vo, T.T., Howerton, K., Larocque, N., Fisher, S.J., Schlaepfer, D.D., and Ilic, D. (2008). Nuclear FAK promotes cell proliferation and survival through FERM-enhanced p53 degradation. *Mol. Cell* 29, 9–22.
- Lim, S.T., Chen, X.L., Tomar, A., Miller, N.L., Yoo, J., and Schlaepfer, D.D. (2010a). Knock-in mutation reveals an essential role for focal adhesion kinase activity in blood vessel morphogenesis and cell motility-polarity but not cell proliferation. *J. Biol. Chem.* 285, 21526–21536.
- Lim, S.T., Miller, N.L., Nam, J.O., Chen, X.L., Lim, Y., and Schlaepfer, D.D. (2010b). Pyk2 inhibition of p53 as an adaptive and intrinsic mechanism facilitating cell proliferation and survival. *J. Biol. Chem.* 285, 1743–1753.
- Mitra, S.K., Hanson, D.A., and Schlaepfer, D.D. (2005). Focal adhesion kinase: in command and control of cell motility. *Nat. Rev. Mol. Cell Biol.* 6, 56–68.
- Nelson, W.J. (2008). Regulation of cell-cell adhesion by the cadherin-catenin complex. *Biochem. Soc. Trans.* 36, 149–155.
- Palka-Hamblin, H.L., Gierut, J.J., Bie, W., Brauer, P.M., Zheng, Y., Asara, J.M., and Tyner, A.L. (2010). Identification of beta-catenin as a target of the intracellular tyrosine kinase PTK6. *J. Cell Sci.* 123, 236–245.
- Pasapera, A.M., Schneider, I.C., Rericha, E., Schlaepfer, D.D., and Waterman, C.M. (2010). Myosin II activity regulates vinculin recruitment to focal adhesions through FAK-mediated paxillin phosphorylation. *J. Cell Biol.* 188, 877–890.
- Piedra, J., Miravet, S., Castaño, J., Pálmer, H.G., Heisterkamp, N., García de Herreros, A., and Duñach, M. (2003). p120 Catenin-associated Fer and Fyn tyrosine kinases regulate beta-catenin Tyr-142 phosphorylation and beta-catenin-alpha-catenin Interaction. *Mol. Cell. Biol.* 23, 2287–2297.
- Plaza-Menacho, I., Morandi, A., Mologni, L., Boender, P., Gambacorti-Passerini, C., Magee, A.I., Hofstra, R.M., Knowles, P., McDonald, N.Q., and Isacke, C.M. (2011). Focal adhesion kinase (FAK) binds RET kinase via its FERM domain, priming a direct and reciprocal RET-FAK transactivation mechanism. *J. Biol. Chem.* 286, 17292–17302.
- Quadri, S.K. (2011). Cross talk between focal adhesion kinase and cadherins: Role in regulating endothelial barrier function. *Microvasc. Res.*, in press.
- Roberts, W.G., Ung, E., Whalen, P., Cooper, B., Hulford, C., Autry, C., Richter, D., Emerson, E., Lin, J., Kath, J., et al. (2008). Antitumor activity and pharmacology of a selective focal adhesion kinase inhibitor, PF-562,271. *Cancer Res.* 68, 1935–1944.
- Roura, S., Miravet, S., Piedra, J., García de Herreros, A., and Duñach, M. (1999). Regulation of E-cadherin/Catenin association by tyrosine phosphorylation. *J. Biol. Chem.* 274, 36734–36740.
- Shen, T.-L., Park, A.Y.J., Alcaraz, A., Peng, X., Jang, I., Koni, P., Flavell, R.A., Gu, H., and Guan, J.-L. (2005). Conditional knockout of focal adhesion kinase in endothelial cells reveals its role in angiogenesis and vascular development in late embryogenesis. *J. Cell Biol.* 169, 941–952.
- Tavora, B., Batista, S., Reynolds, L.E., Jadeja, S., Robinson, S., Kostourou, V., Hart, I., Fruttiger, M., Parsons, M., and Hodivala-Dilke, K.M. (2010). Endothelial FAK is required for tumour angiogenesis. *EMBO Mol. Med.* 2, 516–528.
- Thennes, T., and Mehta, D. (2011). Heterotrimeric G proteins, focal adhesion kinase, and endothelial barrier function. *Microvasc. Res.*, in press.
- Tominaga, J., Fukunaga, Y., Abelardo, E., and Nagafuchi, A. (2008). Defining the function of beta-catenin tyrosine phosphorylation in cadherin-mediated cell-cell adhesion. *Genes Cells* 13, 67–77.
- Wang, Y., Jin, G., Miao, H., Li, J.Y., Usami, S., and Chien, S. (2006). Integrins regulate VE-cadherin and catenins: dependence of this regulation on Src, but not on Ras. *Proc. Natl. Acad. Sci. USA* 103, 1774–1779.
- Weis, S., Cui, J., Barnes, L., and Cheresch, D. (2004a). Endothelial barrier disruption by VEGF-mediated Src activity potentiates tumor cell extravasation and metastasis. *J. Cell Biol.* 167, 223–229.
- Weis, S., Shintani, S., Weber, A., Kirchmair, R., Wood, M., Cravens, A., McSharry, H., Iwakura, A., Yoon, Y.S., Himes, N., et al. (2004b). Src blockade stabilizes a Flk/cadherin complex, reducing edema and tissue injury following myocardial infarction. *J. Clin. Invest.* 113, 885–894.
- Weis, S.M., and Cheresch, D.A. (2005). Pathophysiological consequences of VEGF-induced vascular permeability. *Nature* 437, 497–504.
- Weis, S.M., Lim, S.T., Lutu-Fuga, K.M., Barnes, L.A., Chen, X.L., Göthert, J.R., Shen, T.L., Guan, J.L., Schlaepfer, D.D., and Cheresch, D.A. (2008). Compensatory role for Pyk2 during angiogenesis in adult mice lacking endothelial cell FAK. *J. Cell Biol.* 181, 43–50.
- Wu, L., Bernard-Trifilo, J.A., Lim, Y., Lim, S.T., Mitra, S.K., Uryu, S., Chen, M., Pallen, C.J., Cheung, N.K., Mikolon, D., et al. (2008). Distinct FAK-Src activation events promote alpha5beta1 and alpha4beta1 integrin-stimulated neuroblastoma cell motility. *Oncogene* 27, 1439–1448.
- Wu, M.H., Guo, M., Yuan, S.Y., and Granger, H.J. (2003). Focal adhesion kinase mediates porcine venular hyperpermeability elicited by vascular endothelial growth factor. *J. Physiol.* 552, 691–699.
- Zhao, X., Peng, X., Sun, S., Park, A.Y., and Guan, J.L. (2010). Role of kinase-independent and -dependent functions of FAK in endothelial cell survival and barrier function during embryonic development. *J. Cell Biol.* 189, 955–965.